Journal of The Electrochemical Society, **164** (7) D457-D462 (2017)
0013-4651/2017/164(7)/D457/6/$37.00 © The Electrochemical Society

Impurity Incorporation in the Cu Electrodeposit and Its Effects on the Microstructural Evolution of the Sn/Cu Solder Joints

Hsuan Lee,[a] Tai-Yi Yu,[a] Hsi-Kuei Cheng,[b] Kuo-Chio Liu,[b] Po-Fan Chan,[a] Wei-Ping Dow,[a,*,z] and Chih-Ming Chen[a,z]

[a]*Department of Chemical Engineering, National Chung Hsing University, Taichung 402, Taiwan*
[b]*Backend Operation Division, Taiwan Semiconductor Manufacturing Company, Ltd., Taiwan*

Impurity incorporation in the Cu electrodeposits as a result of the addition of organic additives in the Cu plating solution is investigated with four additive formulas. A common suppressor (polyethylene glycol, PEG) and chloride ions (Cl^-) are added in the plating solution as a control additive formula. Three organosulfides, 3-mercaptopropanesulfonsäure (MPS), bis(3-sulfopropyl) disulfide (SPS), and 3-(2-benzthiazolylthio)-1-propanesulfonsäure (ZPS), are used as accelerators and individually formulated with PEG and Cl^- as the other three experimental formulas. The additive formulas of PEG + Cl^- and PEG + Cl^- + ZPS result in high-level impurity incorporation and cause the microstructural instability of the Sn/Cu joints during thermal aging. Voids and Cu-impurity compounds (CuO and CuS_2) are formed accompanying the growth of the intermetallic compounds (Cu_6Sn_5 and Cu_3Sn) which severely degrades the Sn/Cu joints mechanically. When the additive formulas are changed to PEG + Cl^- + MPS and PEG + Cl^- + SPS, the impurity incorporation is significantly suppressed and thereby inhibits the formation of voids and Cu-impurity compounds. The strong dependence of additive formulas on the impurity incorporation is attributable to the delicate interaction (adsorption competition) between suppressor (PEG) and various accelerators, in which the molecular structures of the organosulfides play a key role.

Manuscript submitted March 15, 2017; revised manuscript received May 11, 2017. Published May 25, 2017.

Cu electroplating is an important technique in microelectronic industries because it offers a cost-effective and reliable method in fabricating the metallizations and interconnects on printed-circuit boards (PCBs) and integrated-circuit (IC) Si chips.[1–10] With the rapid development toward miniaturization, portability, and multi-functionality for microelectronics, the dimensions of the Cu metallizations/interconnects need to reduce significantly to meet the scale down of the packaging structures. The geometrical complexity of the Cu electrodeposits also increases due to the development of three-dimensional high-density interconnect (HDI) and through-silicon-via (TSV) technologies.[1–4] The dimensional scale-down and geometrical complexity bring about new challenges to the Cu electroplating technique. Careful modification of the Cu plating formulas has been proven to be a useful method to overcome the deposition difficulties resulting from the issues of dimension and geometry.[5–10]

In addition to basic electrolytes (Cu sulfate and sulfuric acid), several functional organic additives are added in the Cu plating solution for specific plating processes such as micro-via filling.[5–10] A basic requirement for successful micro-via filling is free of voids in the micro-vias during bottom-up filling and superfilling,[5–8] and this requires a synergy resulting from the organic additives.[5–11] Typical additives include a suppressor, an accelerator, and a leveler. A common suppressor is composed of polyethylene glycol (PEG) and chloride ions (Cl^-) which can chelate with the Cu ions from the plating solution to form a PEG-Cu^+-Cl^- complex, thereby suppressing the Cu deposition rate.[12] An accelerator is composed of a sulfur-containing compound like bis(3-sulfopropyl) disulfide (SPS) and chloride ions. The accelerating effect relies on the molecular structure of the organosulfide which contains two specific functional groups, i.e., a head adsorbing group (disulfide) for effective adsorption on the Cu electrodeposit and a terminal anion group (sulfonic acid) for attracting the Cu ions from the plating solution.[8,10,13–15] Moffat et al.[16] and Magnussen et al.[17] had studied the adsorption mechanism of accelerator using in-situ scanning tunneling microscopy (STM).

Sn-containing solders are extensively used as the joining materials to connect different levels of circuitry on PCBs or IC chips and, therefore, numerous Sn/Cu joints are formed in the microelectronic products. Two intermetallic compounds (IMCs), Cu_6Sn_5 and Cu_3Sn, are formed at the Sn/Cu interface as a result of the Sn/Cu interfacial reaction upon joining.[18–20] Kirkendall voids are frequently formed in the IMCs due to an imbalance of atomic fluxes between Sn and Cu.[21–25] In general, the use of organic additives in the Cu plating solution inevitably results in the incorporation of impurities (carbon, sulfur, chlorine, and oxygen originating from the organic additives) in the Cu electrodeposits. However, a high level of impurity incorporation leads to excessive impurity segregation at the Sn/Cu interface and induces massive void formation in the IMCs which causes more severe reliability problems.[26–29]

Previous studies have reported that the cause of high-level impurity incorporation is fairly complicated, in which additive formula, plating current density, and bath aging are all influential.[26–35] A brief summary of related literatures published by Dimitrov et al.[27,28] indicates that the use of only suppressor (PEG + Cl^-) is prone to high-level impurity incorporation, but the use of both suppressor and accelerator (PEG + SPS + Cl^-) results in a synergistic effect capable of preventing the organic additives from incorporating in the Cu electrodeposits, thereby suppressing the void formation at the Sn/Cu interface.[20,27–29] Ho et al.[36] indicated that the impurities accumulated at the Cu surface during the self-annealing process, and high-speed electrodeposition of Cu leaded to a higher level of impurity incorporation and nanovoid formation.[37]

In addition to SPS, 3-mercaptopropanesulfonsäure (MPS) and 3-(2-benzthiazolylthio)-1-propanesulfonsäure (ZPS) are also typical accelerators with different functional groups;[38] however, their effects on the impurity incorporation/void formation are not investigated yet. In this study, the effects of the three accelerators, SPS, MPS, and ZPS, are systematically examined. The three accelerators are respectively added in the Cu plating solution together with suppressor (PEG + Cl^-) to fabricate the Cu electrodeposits and then join with Sn to perform thermal aging. The results show that SPS and MPS are effective accelerators in conjunction with PEG + Cl^- and are able to suppress the impurity incorporation and void formation, but ZPS is not. The acceleration ability of the accelerators closely correlates with their molecular structures which affect the adsorptive affinity on the growing Cu electrodeposit significantly.

Experimental

The Cu plating process was performed in a Haring cell containing a basic electrolyte (0.88 M $CuSO_4 \bullet 5H_2O$, 0.54 M H_2SO_4, and 1.69 mM NaCl) and organic additives. Polyethylene glycol (PEG, 8000 g/mol, 50 ppm, Fluka, Germany) was added in the plating solution as a suppressor. Three accelerators, MPS (Raschig GmbH, Germany), SPS (Raschig GmbH, Germany), and ZPS (Raschig GmbH, Germany), with a concentration of 2 ppm were used. Overall, there are

*Electrochemical Society Member.
[z]E-mail: chencm@nchu.edu.tw; dowwp@dragon.nchu.edu.tw

four additive formulas for the Cu plating solution. One is with only PEG and Cl^- ions and is denominated as PC, which is used as the control formula without any accelerator. The other three formulas are PC + MPS, PC + SPS, and PC + ZPS, which contain various accelerators in conjunction with the same suppressor (PEG + Cl^-). The plating temperature and current density are 28°C and 32 ASF, respectively. After electroplating, the impurities incorporated in the Cu electrodeposits were quantitatively examined using a secondary ion mass spectrometer (SIMS, ims 4f, CAMECA, France).

Pure Sn shots (99.9%, Showa, Japan) were prepared (22 mg) and joined with the Cu electrodeposits at 260°C for 30 s and then thermally aged at 200°C in a furnace. After 72 h, the Sn/Cu joint samples were ground and polished using SiC sandpapers and Al_2O_3 suspensions, respectively, to expose the cross sections of the Sn/Cu interface for microstructural observation using a field-emission scanning electron microscopy (FE-SEM, JEOLJSM-6700F, Japan). Some selected samples were polished using a focused ion beam (FIB, JIB-4601F, JEOL, Japan) and the resulting cross sections were examined using a FE-SEM and a transmission electron microscopy (TEM, Osiris, FEI, America). The elemental compositions were determined using an energy dispersive spectrometer (EDS, Quantax Super X, Bruker, America) equipped with SEM and TEM. The shear strength of aged joint samples was measured using a bond tester (QC-513, Cometech, Taiwan) with a shear tool speed and shear height of 60 mm/min and 80 μm, respectively.

The acceleration ability of various accelerators was characterized by cyclic voltammetry (CV) which was performed using a potentiostat (PGSTAT30, Auto-Lab) with a three-electrode cell. The working electrode is a polycrystalline Au rotating disk with a diameter of 3 mm, the counter electrode is a Cu bar, and the reference electrode is a saturated mercury-mercurous sulfate electrode. Before CV analysis, the working electrode was polished using a 0.3 μm Al_2O_3 suspension and then cleaned electrochemically by repetitive oxidation-reduction cycles (ORCs) in the range from −0.7 V to 0.9 V in a 0.54 M H_2SO_4 solution to ensure no any contaminations on the Au surface.[10] Subsequently, the working electrode was immersed in a glass cell containing an electrolyte (0.54 M H_2SO_4, 0.88 M $CuSO_4 \cdot 5H_2O$, and 1.084×10^{-4} M organosulfide) for 5 min to form a self-assembled monolayer (SAM) on the working electrode. The organosulfides used here are MPS, SPS, and ZPS. The SAM-coated working electrode was cleaned with deionized water and then immersed in another glass cell containing another electrolyte (0.54 M H_2SO_4, 0.88 M $CuSO_4 \cdot 5H_2O$, 50 ppm PEG, and 60 ppm Cl^-) to perform the CV analysis at 28°C with a scan rate of 5 mV s^{-1}. A control experiment was also performed by immersing a bare working electrode (without a SAM) in the same electrolyte for CV examination. The counter and reference electrodes were placed in two separate salt bridges containing an electrolyte (0.54 M H_2SO_4 and 0.88 M $CuSO_4 \cdot 5H_2O$) and a saturated K_2SO_4 solution, respectively. The open circuit potentials were −0.03 V, −0.03 V, and −0.07 V for MPS, SPS, and ZPS, respectively.

Results and Discussion

Figs. 1a–1d show the cross-sectional SEM micrographs of the Sn/Cu interface after thermal aging at 200°C for 72 h, in which the Cu electrodeposits were prepared using various additive formulas. All the additive formulas contain the same suppressor (PEG + Cl^-, i.e., PC) but different accelerators. Two IMC layers are formed at the Sn/Cu interface. The IMC next to Sn is identified as the Cu_6Sn_5 phase and that next to Cu is the Cu_3Sn phase based on the compositional analysis of EDX. The IMC formation of Cu_6Sn_5 and Cu_3Sn at the Sn/Cu interface subjected to thermal aging is consistent with previous studies.[21,39–41] However, the use of accelerators shows a pronounced effect on the microstructural evolution of the IMC layers. In Figs. 1a and 1b for the additive formulas without accelerator and with ZPS, respectively, the IMCs grow rapidly with the formation of ribbon-like structures in the IMC layers, forming an alternating multi-layer structure. The cross section of the PC sample (Fig. 1a) was further polished using FIB and the ribbon-like structures were zoomed in for

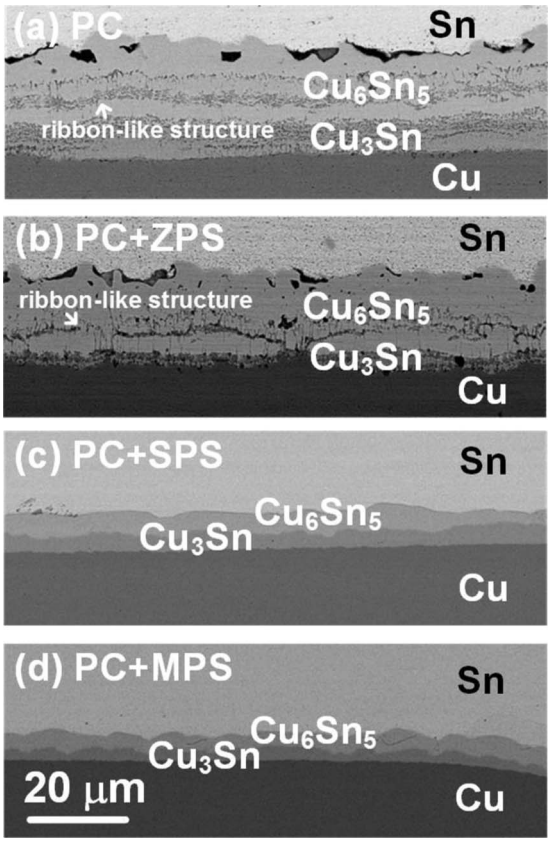

Figure 1. Cross-sectional SEM micrographs of the Sn/Cu interfaces after thermal aging at 200°C for 72 h, where the Cu electrodeposits were prepared using various additive formulas: (a) PC, (b) PC + ZPS, (c) PC + SPS, (d) PC + MPS. (PC refers to PEG and Cl^-).

detailed observation. As shown in Fig. 2, the ribbon-like structures are composed of void and a gray substance. The gray substances are formed dispersedly in the IMC layers and their sizes are too small to precisely detect the compositions using EDX that equips with SEM. So, the sample in Fig. 2 was thinned using FIB for TEM examination.

In the bright-field TEM image shown in Fig. 3a, the gray substance is a little translucent, meaning that it is loose structurally. TEM-EDX analysis shows that the gray, loose substance contains Cu, Sn, S, O, and C (denominated as $Cu_xSn_yS_zO_mC_n$) and their respective composition is listed in the inset table in Fig. 3. The compositions listed in the inset table are average values of three measurements of different locations. In addition to Cu and Sn, the gray, loose substance also contains minor impurities, S, O, and C, which should be a result of the

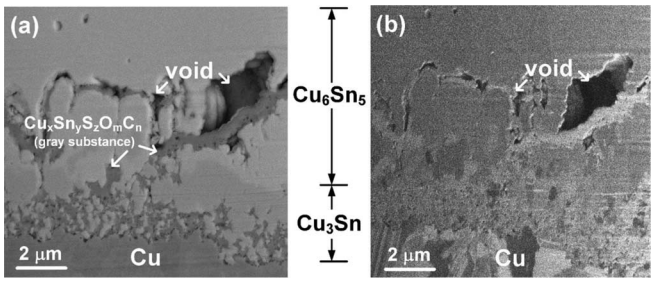

Figure 2. Zoom-in cross-sectional SEM micrograph of the Sn/Cu interface after thermal aging at 200°C for 72 h where the Cu electrodeposit was prepared using PC as the additive formula: (a) backscattered electron image, (b) secondary electron image. (PC refers to PEG and Cl^-).

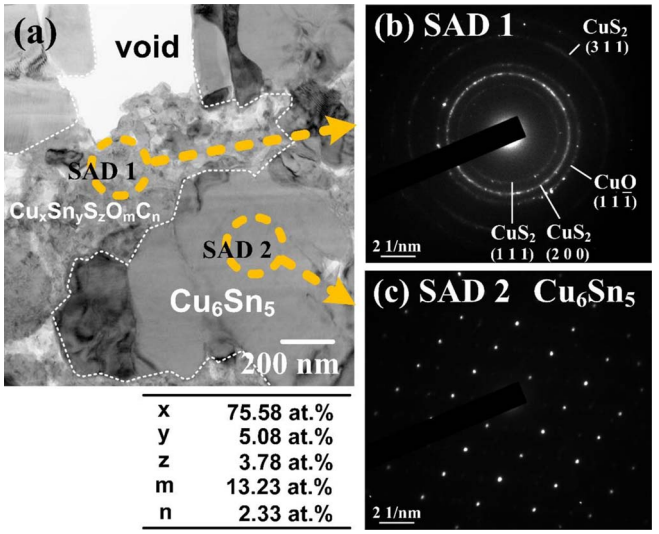

Figure 3. (a) Bright-field TEM image of the ribbon-like structure, (b) Selected area diffraction (SAD) pattern of the Cu-impurity compounds (CuO and CuS_2), (c) SAD pattern of the Cu_6Sn_5 phase.

incorporation of the organic additives in the Cu electrodeposits. The S residue came from the basic electrolyte ($CuSO_4 \bullet 5H_2O$ or H_2SO_4) in the plating solution because no sulfur-containing accelerator was used for the PC formula. The O and C residues might come from the basic electrolyte and PEG. Although Cl was also used for the PC formula, no Cl content was detected which was due to a very low level of incorporation or experimental uncertainty resulting from the confined analytical area of TEM-SAD. The existence of $Cu_xSn_yS_zO_mC_n$ in the IMC layers implies that the impurities originally in the Cu electrodeposit segregate toward the Sn/Cu interface during thermal aging and participate in the growth of the IMCs. Based on the selected area diffraction (SAD) pattern shown in Fig. 3b, the $Cu_xSn_yS_zO_mC_n$ compound is not a single phase but is likely to be a mixture primarily containing CuO and CuS_2. This also implies that the impurity O and S have a strong affinity to Cu, so O and S react with Cu to form the CuO and CuS_2 phase, respectively. Although Cu may react with oxygen in the atmosphere to form oxides during TEM sample preparation, we believe the formation of CuO in Fig. 3a is a result of impurity incorporation because no Cu oxides were found when the Cu substrate was prepared using casting.[42] In contrast, Sn is relatively inert, so no Sn-impurity compounds are found. Although C is also detected, no carbides are found which may be due to its lower amount (2.33 at.%). The compact grain underneath the $Cu_xSn_yS_zO_mC_n$ compound is the Cu_6Sn_5 phase with a single crystal structure as identified by the SAD pattern shown in Fig. 3c.

The use of SPS and MPS as the accelerators helps restore the microstructural integrity of the IMCs without the formation of ribbon-like structures, as shown in Figs. 1c and 1d, respectively. As usual, a compact bilayer structure of Cu_6Sn_5/Cu_3Sn is formed at the Sn/Cu interface. The microstructural evolution of the IMC layers shown in Fig. 1 closely correlates with the impurity concentration in the

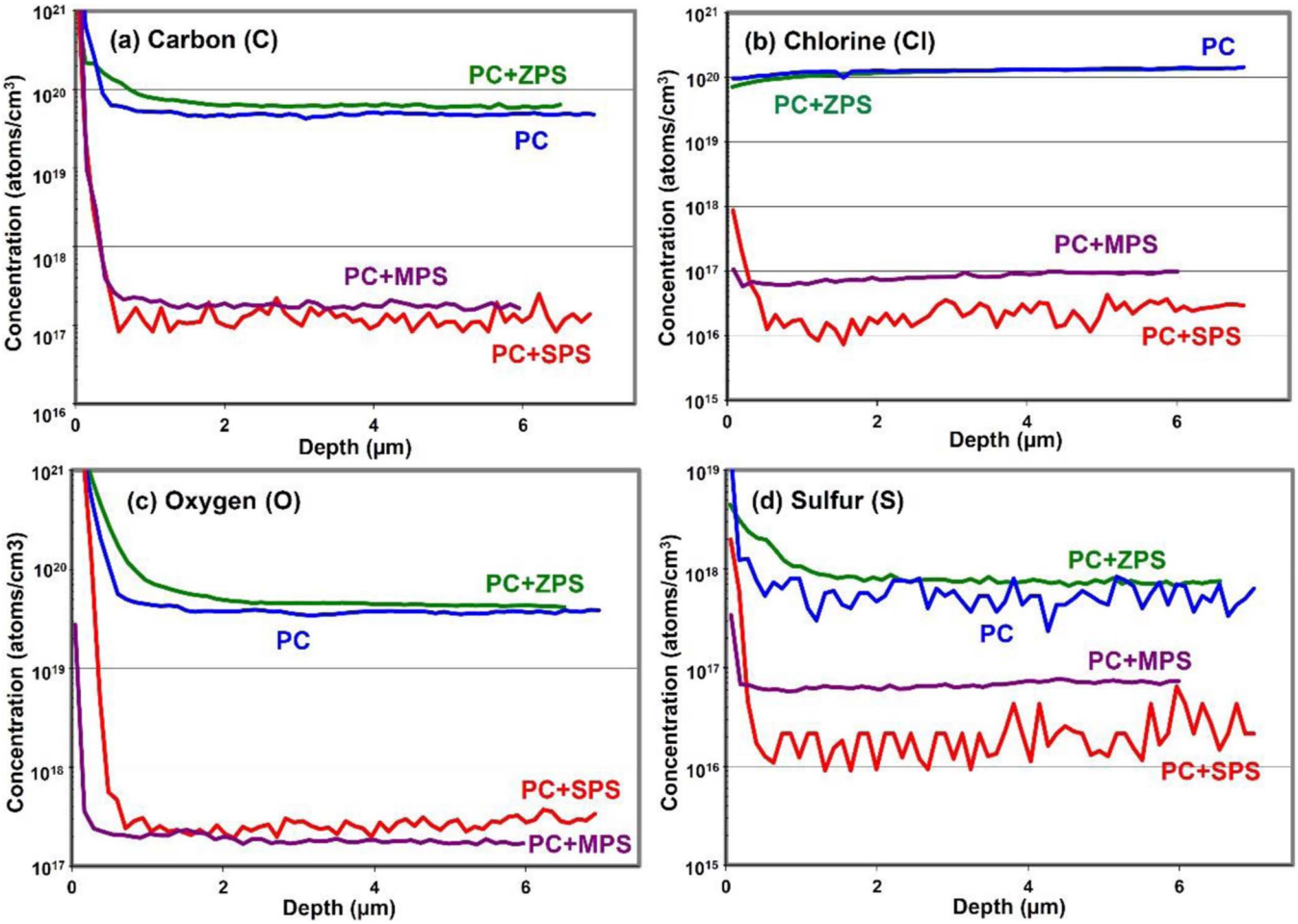

Figure 4. Concentration-depth profiles of the impurities in the Cu electrodeposits prepared with various additive formulas. The impurities are (a) carbon, (b) chlorine, (c) oxygen, and (d) sulfur.

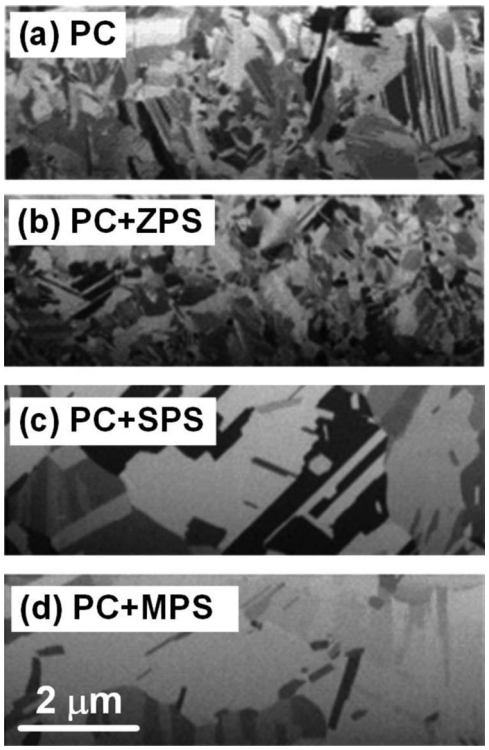

Figure 5. Cross-sectional SEM micrographs of the Cu electrodeposits prepared with various additive formulas: (a) PC, (b) PC + ZPS, (c) PC + SPS, (d) PC + MPS. (PC refers to PEG and Cl^-).

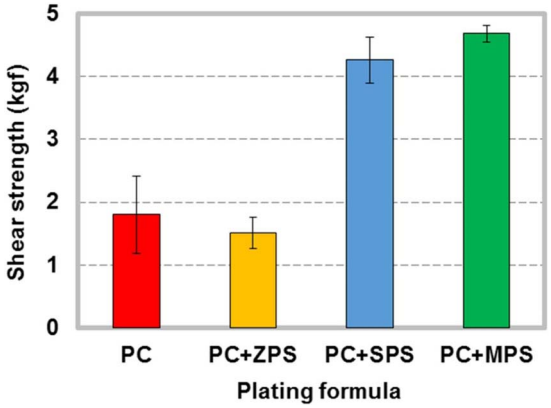

Figure 6. Shear strength of the Sn/Cu solder joints after thermal aging at 200°C for 72 h, where the Cu electrodeposits were prepared using various additive formulas as listed in the transverse axis.

Cu electrodeposits. Fig. 4 shows the concentration-depth profiles of potential impurities (C, Cl, O, and S) in the Cu electrodeposits. It is found that the impurity concentrations in the Cu electrodeposits fabricated using PC and PC + ZPS as the plating formulas are two to three orders of magnitude higher than those fabricated using PC + SPS and PC + MPS. This implies that the unusual alternating multi-layer structure of IMCs is a result of a high level of impurity incorporation in the Cu electrodeposits (PC and PC + ZPS). A strong dependence of the impurity concentration on the grain morphology of the Cu electrodeposits is also found. As shown in Fig. 5, the grain morphologies of the two Cu electrodeposits (PC and PC + ZPS) are similar and the grain sizes are much smaller than those of the other two Cu electrodeposits (PC + SPS and PC + MPS). Because the grain boundaries are potential sites for the impurity incorporation,[20,43-45] the two Cu electrodeposits (PC and PC + ZPS) are prone to have a higher level of impurity incorporation due to their higher grain boundary density. In contrast, the other two Cu electrodeposits (PC + SPS and PC + MPS) have a lower grain boundary density and, therefore, a lower level of impurity incorporation, which is in good agreement with the SIMS results shown in Fig. 4.

The microstructural instability of the solder joints due to impurity incorporation was also observed in the Sn-3.5 Ag/Cu solder joints[22,23] where the Cu substrate was plated using only SPS as additive. Voids are formed massively along the Cu_3Sn/Cu interface as a result of sulfur segregation originating from SPS. The interfacial voids interfere significantly the atomic interdiffusion between Sn and Cu which causes the IMCs to periodically form accompanying new void formation. As a result, the microstructural integrity of the solder joint collapses and evolves into an alternating multi-layer structure composed of repeated IMC/void pairs.

Previous studies have suggested a possible mechanism for accelerated void formation in the presence of impurities,[20,27–29] in which the impurity residues block the vacancy annihilation sites (e.g. grain boundary and dislocation) and cause vacancy supersaturation to form voids. Here, we find that the impurities not only accelerate the void formation but also react with Cu to form the CuO and CuS_2 compounds embedded in the IMC layers (Fig. 2). To the best of our knowledge, the report of the Cu-impurity compound formation in the Sn/Cu interfacial reaction due to impurity incorporation is rare.[42] This specular finding opens a new research direction and reminds the microelectronic researchers to pay special attention to the solder joints involving with the Cu electroplating process. The CuO and CuS_2 compounds might play a role of heterogeneous nucleation site to accelerate the IMC growth as seen in Figs. 1a and 1b. Elimination of vacancy sinks due to impurity segregation also releases vacancies and facilitates the atomic diffusion, thereby enhancing the IMC growth. However, excessive IMC growth and formation of the void/Cu-impurity compounds are detrimental to the mechanical property of the solder joints due to high microstructural instability. As shown in Fig. 6, when an alternating multi-layer structure is formed at the Sn/Cu interface (for the additive formulas of PC and PC + ZPS), the shear strength dramatically drops by over 50% in comparison with a compact bi-layer structure of Cu_6Sn_5 and Cu_3Sn (for the additive formulas of PC + SPS and PC + MPS).

Typically, an accelerator contains a head group and a terminal group that can chemically adsorb on the growing Cu surface and attract the Cu^{2+} ions in the plating solution, respectively.[10] Its acceleration ability on Cu electrodeposition depends upon the performance of the two functional groups in the Cu plating process which can be characterized through CV analysis.[10,11] The terminal functional group attracts the Cu^{2+} ions from the plating solution and then the Cu^{2+} ions are transferred to the Cl^- ions that are adsorbed on the Cu deposit, thereby accelerating the Cu deposition. The acceleration process simultaneously accompanies the transfer of floatable organosulfides from the surface of the SAM-modified Au electrode onto the perimeter of the as-deposited Cu surface.[10] A characteristic reduction peak (α) in the CV pattern will be formed in response to the floatability and transferability of the organosulfides and can be taken as an indicator of effective accelerator.[10] Fig. 7 shows the CV curves of the three organosulfides-modified Au electrodes (PC + MPS, PC + SPS, and PC + ZPS) and one bare Au electrode (PC), where only the reduction portion is presented to check the existence of the α peak. The α peak only appears for the two organosulfides (PC + SPS and PC + MPS), showing that SPS and MPS are effective accelerators in the electrolyte (0.54 M H_2SO_4, 0.88 M $CuSO_4$, 50 ppm PEG, and 60 ppm Cl^-). In contrast, the additive formulas of PC and PC + ZPS have no accelerating effect due to the absence of α peak.

Fig. 8 schematically shows the molecular structures of the three organosulfides used as accelerators in the present study. All organosulfides contain a terminal sulfonic acid (SO_3^-) group that can attract the Cu^{2+} ions in the plating solution while the head groups are different. As shown in Fig. 7, SPS and MPS are identified as effective

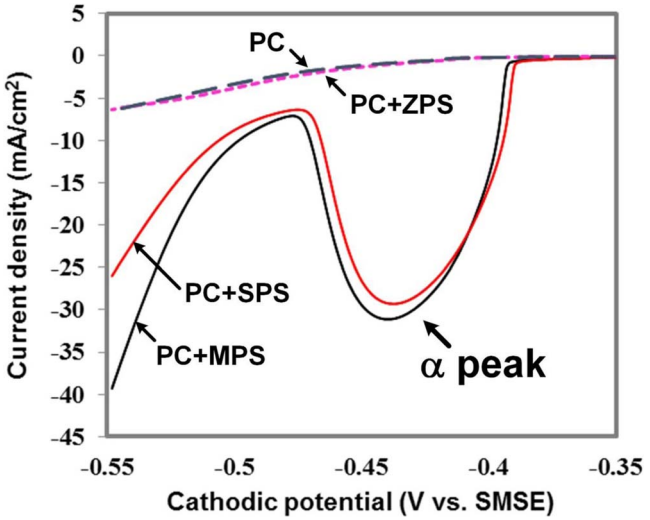

Figure 7. Cyclic voltammograms of the three organosulfides-modified Au electrodes (PC + MPS, PC + SPS, and PC + ZPS) and one bare Au electrode (PC) in an electrolyte containing 0.88 M $CuSO_4$, 0.54 M H_2SO_4, 50 ppm PEG, and 60 ppm Cl^-. Only the reduction portion is presented to check the existence of the α peak.

accelerators due to their α peaks. This can be attributed to their disulfide (R-S-S-R) and thiol (R-S-H) group as shown in Figs. 8b and 8c respectively, that have strong affinity to the deposit surface.[46] The two functional groups also provide dynamic adsorption for the organosulfides on the growing Cu electrodeposits which plays a crucial role for accelerated electrodeposition.[10] The competitive adsorption between effective accelerators (SPS and MPS) and suppressor (PEG) generates a synergistic effect capable of mutually preventing each other from incorporating into the Cu electrodeposits and accordingly suppresses the incorporation of impurities.[28] Therefore, voids and Cu-impurity compounds are absent which retains the microstructural integrity of the IMC layers as shown in Figs. 1c and 1d. In contrast, ZPS is a weak accelerator because its benzothiazolyl head group (Fig. 8a) is a geometrical barrier against its efficient adsorption on the Cu surface.[38] On the other hand, the concentration of ZPS adsorbed onto the Cu deposit may be too low to effectively accelerate the Cu deposition. As a result, the acceleration effect of ZPS is weaker and fails to compete with the suppressor (PEG) on the Cu deposition. However, increment of ZPS concentration may be a possible way to enhance its acceleration effect, but this part needs more investigations and is a goal of our feature research.

Conclusions

The Cu plating formulas, specifically the additive formulas, have a remarkable effect on the impurity incorporation and grain microstructure in the Cu electrodeposits. For the additive formula with only a suppressor, i.e., PC + Cl^-, the Cu electrodeposit exhibits a fine grain microstructure with a high level of impurity incorporation. The incorporated impurities (carbon, sulfur, oxygen, chlorine) segregate toward the Sn/Cu interface during thermal aging at 200°C which induces the formation of voids and the Cu-impurity compounds (CuO and CuS_2) in the Cu_6Sn_5 and Cu_3Sn phase layers, severely destroying the microstructural integrity and the mechanical strength of the Sn/Cu joint. When ZPS is formulated with PC and Cl^-, the formation of voids and the Cu-impurity compounds at the Sn/Cu interface is still observed as a result of a high level of impurity incorporation. The CV analysis indicates that ZPS is a weak accelerator and this may be because its benzothiazolyl head group acts as a geometrical barrier which hinders effective adsorption on the growing Cu electrodeposit. In contrast, MPS and SPS are identified as effective accelerators by the CV analysis and their use in the plating solution together with PC and Cl^- effectively suppresses the impurity incorporation and, therefore, restores the Sn/Cu joints to a stable Cu_6Sn_5/Cu_3Sn bilayer structure without the formation of voids and the Cu-impurity compounds. The acceleration ability is attributed to the disulfide (R-S-S-R) and thiol (R-S-H) functional groups of SPS and MPS, respectively, which can effectively adsorb on the growing Cu electrodeposits and compete with the PEG molecules to suppresses the impurity incorporation.

Acknowledgments

This work is supported in part by the Ministry of Science and Technology of Taiwan (NSC 102-2221-E-005-009-MY3 & MOST-105-2221-E-005-087) and in part by the Taiwan Semiconductor Manufacturing Company, Hsinchu, Taiwan.

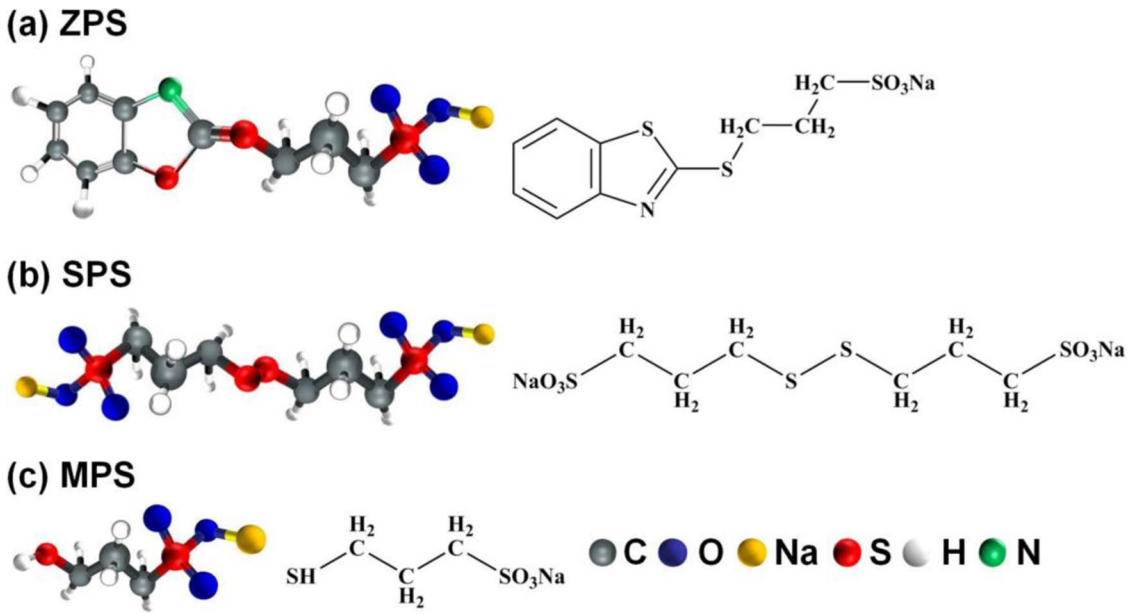

Figure 8. Schematics of the molecular structures of (a) ZPS, (b) SPS, and (c) MPS.

References

1. P. C. Andricacos, C. Uzoh, J. O. Dukovic, J. Horkans, and H. Deligianni, *IBM J. Res. Dev.*, **42**, 567 (1998).
2. P. C. Andricacos, *Electrochem. Soc. Interface*, **8**, 32 (1999).
3. R. Beica, C. Sharbono, and T. Ritzdorf, *IEEE Electron. Compt. Technol. Conf. 58th*, **577** (2008).
4. V. Luo, X. T. Xue, K. C. Yu, J. Meng, H. L. Lu, and D. W. Zhang, *J. Electrochem. Soc.*, **163**, E39 (2016).
5. T. P. Moffat and D. Josell, *J. Electrochem. Soc.*, **159**, D208 (2012).
6. J. J. Sun, K. Kondo, T. Okamura, S. Oh, M. Tomisaka, H. Yonemura, M. Hoshino, and K. Takahashi, *J. Electrochem. Soc.*, **150**, G355 (2003).
7. W. P. Dow, M. Y. Yen, W. B. Lin, and S. W. Ho, *J. Electrochem. Soc.*, **152**, C769 (2005).
8. N. T. M. Hai, V. Grimaudo, P. Moreno-García, and P. Broekmann, *ECS Transactions*, **69**, 57 (2015).
9. G. Y. Lin, J. J. Yan, M. Y. Yen, W. P. Dow, and S. M. Huang, *J. Electrochem. Soc.*, **160**, D3028 (2013).
10. Y. D. Chiu and W. P. Dow, *J. Electrochem. Soc.*, **160**, D3021 (2013).
11. Y. D. Chiu, W. P. Dow, K. Krug, Y. F. Liu, Y. L. Lee, and S. L. Yau, *Langmuir*, **28**, 14476 (2012).
12. Z. V. Feng, X. Li, and A. A. Gewirth, *J. Phys. Chem. B*, **107**, 9415 (2003).
13. M. Tan and J. N. Harb, *J. Electrochem. Soc.*, **150**, C420 (2003).
14. M. Tan, C. Guymon, D. R. Wheeler, and J. N. Harb, *J. Electrochem. Soc.*, **154**, D78 (2007).
15. Y. Jin, Y. Sui, L. Wen, F. Ye, M. Sun, and Q. Wang, *J. Electrochem. Soc.*, **160** D20 (2013).
16. T. P. Moffat and L. Y. O. Yang, *J. Electrochem. Soc.*, **157**, D228 (2010).
17. Y. C. Yang, A. Taranovskyy, and O. M. Magnussen, *Langmuir*, **28**, 14143 (2012).
18. S. W. Chen, C. M. Chen, and W. C. Liu, *J. Electron. Mater.*, **27**, 1193 (1998).
19. C. P. Lin, C. M. Chen, and Y. W. Yen, *J. Alloys Compd.*, **591**, 297 (2014).
20. J. Y. Wu, H. Lee, C. H. Wu, C. F. Lin, W. P. Dow, and C. M. Chen, *J. Electrochem. Soc.*, **161**, D522 (2014).
21. S. Kumar, C. A. Handwerker, and M. A. Dayananda, *J. Phase Equilib. Diff.*, **32**, 309 (2011).
22. J. Y. Kim, J. Yu, and S. H. Kim, *Acta Mater.*, **57**, 5001 (2009).
23. S. H. Kim and J. Yu, *J. Mater. Res.*, **25**, 1854 (2010).
24. T. C. Chiu, K. Zeng, R. Stierman, D. Edwards, and K. Ano, *IEEE Electron. Compt. Technol. Conf. 54th*, 1256 (2004).
25. P. Borgesen, L. Yin, and P. Kondos, *Microelectron. Reliab.*, **52**, 1121 (2012).
26. J. Yu and J. Y. Kim, *Acta Mater.*, **56**, 5514 (2008).
27. Y. Liu, J. Wang, L. Yin, P. Kondos, C. Parks, P. Borgesen, D. Henderson, E. Cotts, and N. Dimitrov, *J. Appl. Electrochem.*, **38**, 1695 (2008).
28. Y. Liu, L. Yin, S. Bliznakov, P. Kondos, P. Borgesen, D. W. Henderson, C. Parks, J. Wang, E. J. Cotts, and N. Dimitrov, *IEEE Trans. Compon. Pack. Technol.*, **33**, 127 (2010).
29. L. Yin and P. Borgesen, *J. Mater. Res.*, **26**, 455 (2011).
30. M. Stangl, J. Acker, S. Oswald, M. Uhlemann, T. Gemming, S. Baunack, and K. Wetzig, *Microelectron. Eng.*, **84**, 54 (2007).
31. J. Kelly, C. Parks, J. Demarest, J. Li, and C. Penny, Springer New York, 115 (2014).
32. M. Y. Cheng, K. W. Chen, T. F. Liu, Y. L. Wang, and H. P. Feng, *Thin Solid Films*, **518**, 7468 (2014).
33. Q. Huang, A. Avekians, S. Ahmed, C. Parks, B. Baker-O'Neal, S. Kitayaporn, A. Sahin, Y. Sun, and T. Cheng, *J. Electrochem. Soc.*, **161**, D388 (2014).
34. S. Kitayaporn, Q. Huang, M. Hopstaken, and B. Baker-O'Neal, *J. Electrochem. Soc.*, **162**, D74 (2015).
35. S. H. Brongersma, E. Kerr, I. Vervoort, A. Saerens, and K. Maex, *Journal of Mater. Res.*, **17**, 582 (2002).
36. C. C. Chen, C. H. Yang, Y. S. Wu, and C. E. Ho, *Surface and Coatings Technology*, (2016).
37. P. T. Lee, Y. S. Wu, P. C. Lin, C. C. Chen, W. Z. Hsieh, and C. E. Ho, *Surface and Coatings Technology*, (2016).
38. T. C. Chen, Y. L. Tsai, C. F. Hsu, W. P. Dow, and Y. Hashimoto, *Electrochim. Acta*, **212**, 572 (2016).
39. T. Y. Lee, W. J. Choi, K. N. Tu, J. W. Jang, S. M. Kuo, J. K. Lin, D. R. Frear, K. Zeng, and J. K. Kivilahti, *J. Mater. Res.*, **17**, 291 (2002).
40. X. Deng, G. Piotrowski, J. J. Williams, and N. Chawla, *J. Electron. Mater.*, **32**, 1403 (2003).
41. Y. Yuan, Y. Guan, D. Li, and N. Moelans, *J. Alloys and Compd.*, **661**, 282 (2016).
42. T. Y. Yu, H. Lee, H. L. Hsu, W. P. Dow, H. K. Cheng, K. C. Liu, and C. M. Chen, *J. Electrochem. Soc.*, **163**, D734 (2016).
43. S. Nakahara, Y. Okinaka, and H. K. Straschil, *J. Electrochem. Soc.*, **136**, 1120 (1989).
44. G. D. Hibbard, J. L. McCrea, G. Palumbo, K. T. Aust, and U. Erb, *Scripta Mater.*, **47**, 83 (2002).
45. Y. M. Wang, S. Cheng, Q. M. Wei, E. Ma, T. G. Nieh, and A. Hamza, *Scripta Mater.*, **51**, 1023 (2004).
46. J. P. Healy, D. Pletcher, and M. Goodenough, *J. Electroanal. Chem.*, **338**, 167 (1992).